Breakdown Mechanisms of Rod-Plane Air Gaps with a Dielectric Barrier Subject to Lightning Impulse Stress

Meyer, H.K.H; Mauseth, F.; Pedersen, A.; Ekeberg, J.

Breakdown mechanisms of rod-plane air gaps with a dielectric barrier subject to lightning impulse stress

Hans Kristian Meyer, Frank Mauseth
Norwegian University of Science and Technology (NTNU)
Department of Electric Power Engineering
Trondheim, Norway

Atle Pedersen
SINTEF Energy Research
Trondheim, Norway

and **Jonas Ekeberg**
ABB Ltd.
Baden-Dättwil, Switzerland

ABSTRACT

The complexity of gas-insulated substations makes it difficult to predict withstand voltages. Modeling interaction between dielectric surfaces and electrical discharges is a key challenge. In this study, 60 mm rod-plane air gaps with a dielectric barrier 20 mm below the rod are stressed with lightning impulses of both polarities. The discharge mechanisms are investigated with a high-speed camera, a photomultiplier tube and a current measurement system. The discharge development and current-velocity relationship is leader-like. With positive polarity applied, a leader propagates from the upper parts of the rod to ground. Negative impulses are characterized by positive leader development from the ground plane to the rod. For both polarities, the discharge starts with streamers propagating from the rod to the barrier. Positive streamers typically reach the opposite electrode without causing breakdown directly. The findings imply that empirical breakdown prediction models for short air gaps should involve conditions for positive leader initiation and development. The results also show that dielectric barriers increase the breakdown voltage by impeding leader development. The barriers increase the shortest discharge path and shift the point of leader inception further up on the rod.

Index Terms — **dielectric barrier, streamers, leaders, propagation, lightning impulse, rod-plane gap, medium voltage, switchgear insulation**

1 INTRODUCTION

Expected restrictions on the use of sulphur hexafluoride (SF_6) gas in medium voltage (MV) switchgear has triggered research efforts to develop environmentally friendly insulation techniques. SF_6 has a 100-year global warming potential (GWP) of roughly 23900 [1]. Using air as insulation has obvious advantages, but it poses dielectric challenges as the equipment must be compact to meet standardized requirements. The field strengths required to initiate discharges are roughly three times lower in air than in SF_6 [2]. Up to three times greater electrode clearances are therefore needed in air than in SF_6 for similar geometries. Accurate withstand voltage prediction models are therefore needed to optimize the dielectric design. This requires a solid understanding of the physical processes leading to breakdown. These processes are complex and difficult to model accurately, so empirical models are typically used [3], [4]. The models can, however, lead to inaccurate results when the insulation system includes dielectric surfaces. Such surfaces are common in switchgear insulation in the form of shafts, spacers or dielectric barriers. Dielectric barriers can significantly improve the withstand voltage of an air gap [5]–[7], and could therefore be used to design space efficient insulation systems with low environmental impact. The aim of this work is to investigate the influence of dielectric barriers on breakdown development in short air-insulated rod-plane gaps. 1.2/50 µs lightning impulses (LI) are used as they are dimensioning in typical MV switchgear type tests [8].

Manuscript received on 11 September 2017, in final form 1 February 2018, accepted 2 February 2018. Corresponding author: H.K. Hygen.

2 BREAKDOWN OF INHOMOGENEOUS AIR GAPS

2.1 STREAMER INCEPTION

The discharge process of inhomogeneous air gaps begins with an electron avalanche of critical size. The space charge left by the avalanche turns into a filamentary discharge, a *streamer*. One dielectric design strategy is to avoid field strengths capable of initiating streamers. To calculate these field strengths, the streamer inception integral

$$\int_{\Gamma} \alpha\,(E(x))\mathrm{d}x \geq \ln N \tag{1}$$

is used. The field-dependent effective ionization coefficient $\alpha(E(x))$ can be estimated with empirical fit functions [2]. The integral is typically evaluated along a critical field line Γ, where $\alpha > 0$, until a critical background field E_{cr} where $\alpha(E_{\mathrm{cr}}) = 0$ is reached. $E_{\mathrm{cr}} = 2.5$ kV/mm for atmospheric air [9]. Inception occurs when the critical number of electrons exceeds $N = 10^8$ [10]. A design approach based on avoiding inception can, however, be overly cautious as inception does not necessarily lead to breakdown.

2.2 STREAMER PROPAGATION

Streamers require a non-zero background field strength to propagate as they dissipate some energy in the process. Another design approach is therefore to allow inception, but inhibit propagation. Positive withstand voltage $U_{\mathrm{W}} = U_{50\%} - 3\sigma$ [10] of inhomogeneous gaps increases linearly with shortest discharge path x_{S} [3]:

$$U_{\mathrm{W}} = U_0 + E_{\mathrm{st}} x_{\mathrm{S}} \tag{2}$$

where the constant $E_{\mathrm{st}} = 0.5$–0.54 kV/mm can be interpreted as the internal streamer channel field. E_{st} therefore represents the minimum background field required for stable streamer propagation. $U_0 =$ 20–30 kV can be viewed as the excess potential needed to cause breakdown after the streamers have bridged the gap [3].

Propagation of streamers has been explored with fluid simulations, e.g. [11]–[14]. The large computational burden of such models have, however, limited their application so far, especially for 3D.

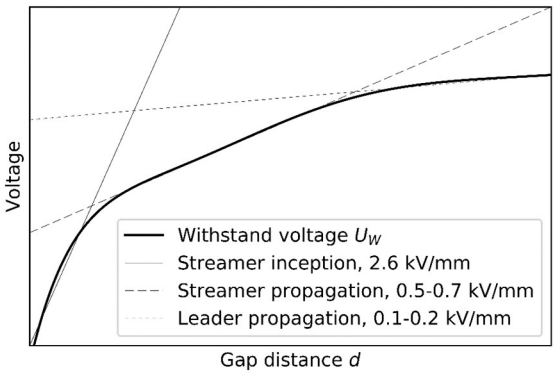

Figure 1. Typical relation between breakdown voltage and gap distance in inhomogeneous fields with fixed radius of curvature [3].

2.3 LEADERS/LEADER-TYPE CHANNELS

Crossing of streamer discharges is not a sufficient condition for breakdown in short rod-plane gaps. Secondary streamer channel heating or "leader-type channels" are needed [15]. Leader-type channels resemble *leaders*, but leaders are traditionally considered to occur in gaps >0.5–1m only [10], [16], [17]. For such large gaps, breakdown voltage typically increases with 0.1–0.2 kV/mm as illustrated in Figure 1. 1.2/50 µs impulse overvoltages are considered too short to support leader breakdown for long gaps due to the slow leader propagation speed (0.02 mm/ns) [16]. A positive leader breakdown typically happens in the following way [17], [18]

1. Primary streamers occur, leaving residual space charges that distort the field distribution
2. Dark period without discharge activity
3. Inception of stems/secondary streamers at the anode
4. Joule heating of stems, leading to temperatures exceeding 1500 K, reduction of gas density
5. Detachment of negative ions due to higher gas temperature. This increases the stem conductivity and field strength at its tip
6. Development of streamers at the stem (leader) front, due to the high field at the leader tip
7. Leader propagation into the gap as Joule heating extends the channel
8. Leader reaching counter-electrode, with subsequent arc

High-speed images of leader-type channels indicate that the above list could apply to leader-type channels as well [15], [19]. The two terms are therefore used interchangeably in the following.

The leader velocity v_{L} depends on the ionization activity at its front, and is typically proportional to leader channel current I_{L} [17], [18]:

$$v_{\mathrm{L}} = \frac{1}{q} I_{\mathrm{L}} \tag{3}$$

where $q =$ 20–50 µC/m represents the average charge necessary for a unit length advancement of the leader channel. The ionization activity depends on the field strength at the channel front, E_{F}, which in turn depends on the applied voltage U and the leader channel field E_{L}. E_{L} decreases with leader length in the range $E_{\mathrm{L}} = 0.5$–0.1 kV/mm, but the reduced field $E_{\mathrm{L}}/n_{\mathrm{n}}$ is constant due to channel expansion and decreasing gas density n_{n}.

2.4 NEGATIVE BREAKDOWN

Less is known about negative lightning impulse breakdown in air. This is partly because positive breakdown occurs at lower voltage magnitudes, and is therefore more critical in high voltage applications. Negative breakdown voltage is higher than positive as negative streamers have less effective propagation mechanisms, and require a higher background field $E_{\mathrm{st}} =$1–1.15 kV/mm [10].

Negative breakdown of longer gaps is known to often involve a system of streamers and leaders of both polarities after the dark period [20]. Typically, the negative leader propagation is driven by *space stems*, bright spots from which streamers of both polarities propagate. A dense network of streamers

Table 1. Rod-plane gap with a dielectric barrier, parameters.

	Parameter	Used
Electrical	Voltage shape	1.2/50 µs LI
	Voltage magnitude U	50-120 kV
	Polarity	Both
	Barrier initial charge	Cleaned (<300 V)
Ambient	Gas mixture	Ambient air
	Temperature (*logged*)	20-24 ºC
	Pressure (*logged*)	0.997 to 1.020 bar
	Rel. humidity (*logged*)	33 to 44 %
	Background radiation	Cosmic
Geometrical	Rod height d	60 mm
	Rod shape	Hemispheric
	Rod radius r	3.5 mm
	Barrier height $d - a$	40 mm
	Barrier overhang b	0-80 mm
	Barrier shape	Square 600x600x5 mm
Material	Barrier material	Polycarbonate (Lexan)
	ϵ_r @ 50 Hz	2.96 [21]
	Surface cond. σ_s	$< 10^{-17}$ Ω^{-1}cm^{-1} [21]
	Bulk cond. σ_B	$< 10^{-17}$ Ω^{-1}cm^{-1} [21]
	Barrier roughness	Unknown
	Electrode material	Aluminum
	Electrode roughness	Unknown

connects the negative leader and stem. These stems can sometimes become leaders, which then approach the main leader with increasing velocity.

2.5 ROD-PLANE GAPS WITH DIELECTRIC BARRIERS

Rod-plane gaps are often used to study effects of field inhomogeneity. While being polarity dependent, it is a simple arrangement, which facilitates analysis and validation of breakdown models. However, there are many parameters involved. As can be seen in Table 1, adding a dielectric barrier introduces at least five new parameters and a history effect if the barrier is not completely discharged between impulses.

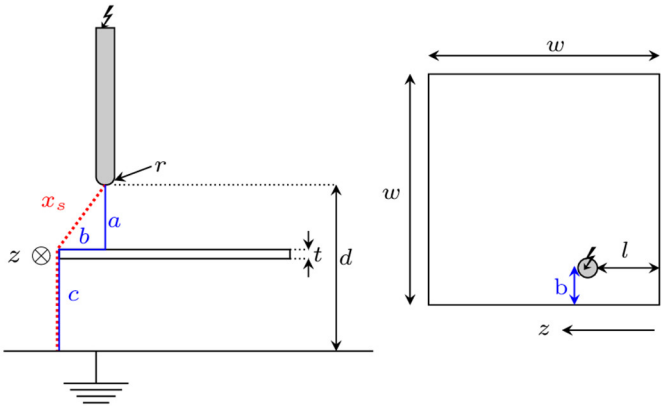

Figure 2. Rod-plane gap with insulating barrier seen from the side and from above. The ratios w/b and l/b were chosen relatively large to ensure that streamer and leader propagation would occur inside the frame and transverse to the camera axis z.

With dielectric barriers in the discharge path, streamers typically propagate along and around the barrier to ground [11], [22]. Barriers can also inhibit secondary streamer development [23], cause leaders to propagate a longer path in the gas phase [24] or stop them [25].

Charges on the barrier will alter the field distribution as shown in Figure 3, with different implications depending on applied voltage and dielectric barrier charge polarity. In Figures 3a and 3b, the rod tip is shielded and the field stress is shifted to the barrier-plane gap. These situations typically occur under DC or during an impulse right after the barrier has been charged by initial streamers. In Figures 3c and 3d, the stress is highest in the rod-barrier gap. These situations can occur during AC or at the declining impulse tail, when the field between the rod and residual charge on the barrier becomes reversed. Reverse discharges from the rod can neutralize charge on the barrier surface in these cases [25].

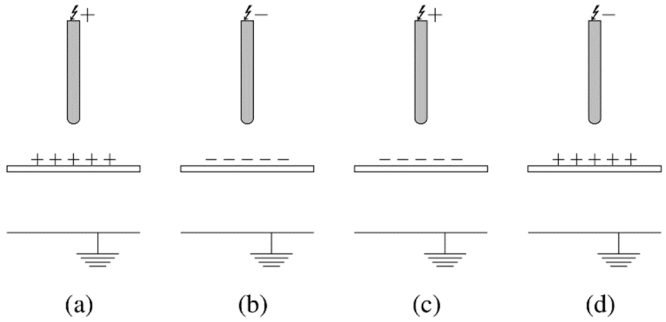

Figure 3. Applied rod voltage and dielectric barrier charge polarity configurations. a) and b) rod voltage same as dielectric barrier charge polarity. c) and d) different polarity between rod and barrier.

3 EXPERIMENTAL

3.1 CAMERA AND PMT

A rod-plane gap with a hemispheric rod tip of radius $r = 3.5$ mm placed 60 mm over a 1x1 m ground plane and 20 mm over a polycarbonate (Lexan) barrier was stressed with 1.2/50 µs lightning impulses using a 1.2 MV impulse generator, see Figure 4. The experiments were performed in ambient air with the temperature, pressure and relative humidity being logged. The barrier was cleaned with isopropyl alcohol between impulses to remove charge. An electrostatic voltmeter was used to verify that this procedure results in a surface potential below 500 V.

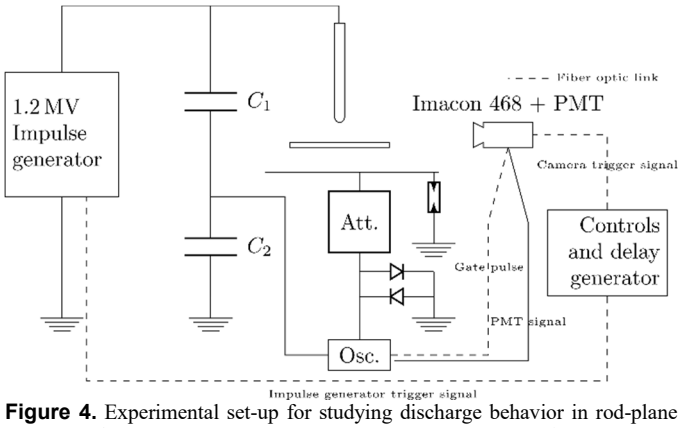

Figure 4. Experimental set-up for studying discharge behavior in rod-plane gaps. Impulse generator, camera, PMT, current measurement using attenuators (Att.) and current measurement protection (spark gaps and diodes) are shown.

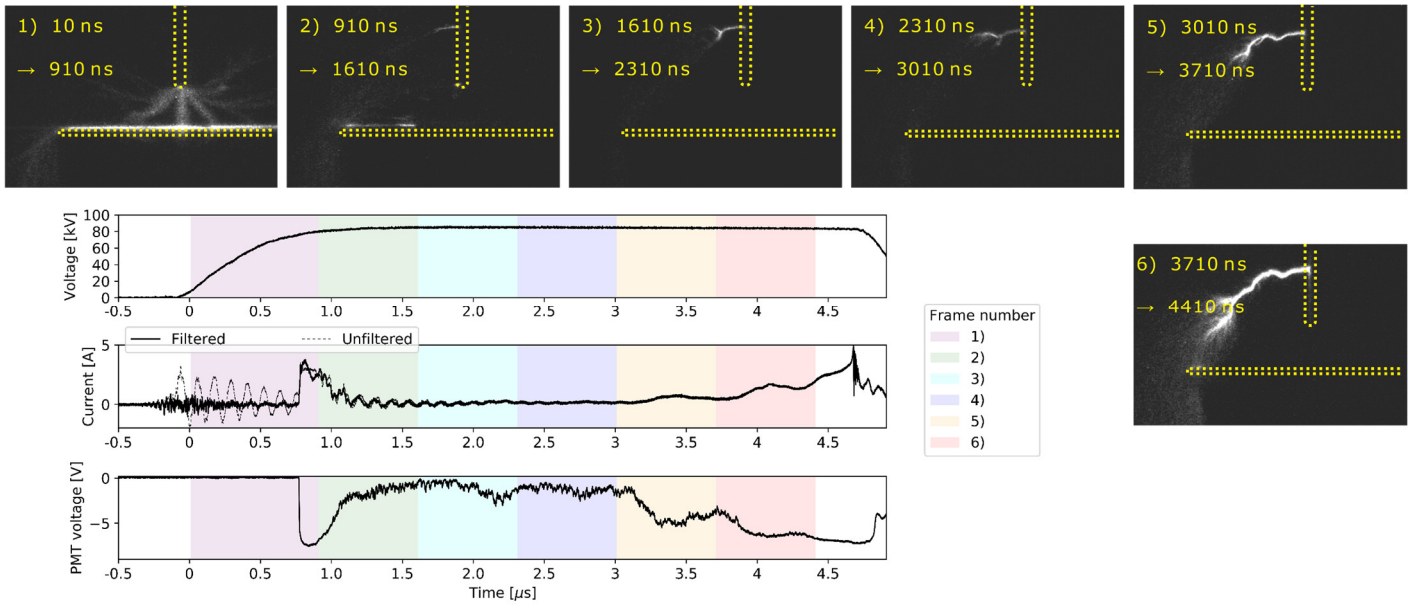

Figure 5. $d = 60$ mm rod-plane gap with barrier at $c = 40$ mm with $b = 60$ mm overhang (see Figure 2), 1.2/50µs LI 86 kV applied. PMT wavelength detection range 495-850 nm.

An Imacon 468 ICCD camera with 7 frames of 10 ns minimum exposure time each was triggered with a delay generator to capture the spatiotemporal discharge development. An 85 mm f/1.8 Nikkor lens was used with the camera which was placed inside a Faraday cage about 1 m away from the rod. A continuous signal of the light intensity was obtained using a PMT about 2 m away. A Philips 56AVP/TVP PMT was used with 2.5 kV supply voltage. A low-pass filter blocking light with wavelength < 495 nm and a paper-layer filter were used in the experimental work to limit PMT saturation. The PMT filter type used is indicated in the figure texts.

3.2 CURRENT MEASUREMENT SYSTEM

The current was measured through a signal cable (RG-214) with bandwidth of about 400 MHz connected to the ground plane. The signal cable was matched at the oscilloscope end after passing through a series of 13 GHz T-type attenuators with a damping of up to 59.8 dB. To protect the oscilloscope from breakdown currents, a 430 V spark gap was placed close to the ground plane, see Figure 4. Two diodes were placed in anti-parallel close to the oscilloscope to arrest the fastest voltage transients. The spark gap voltage or attenuation can be modified to measure different current ranges, but a practical upper limit is given by the thermal rating of the first attenuator, 5000 V for 400 ns.

3.3 DIGITAL POST-PROCESSING

The propagation times in the PMT, current and voltage measurement cables were found using a pulse generator. These cable delays and the internal PMT delay were compensated in the digital post-processing of the oscilloscope recordings. The correct timing of the camera monitor pulse was found using a PMT and a fast light-emitting diode. A Python script that filters out the current measurement noise and capacitive current was made. The script subtracts a scaled measurement where no discharge activity was seen in the gap on the camera or PMT. The original current measurement is also plotted in the results. The same script also integrates the current measurement during each frame to evaluate the validity of equation (3).

As the discharges are faint, the image brightness and contrast were enhanced with photo-editing software. These parameters were adjusted to the same levels in all image series to normalize the evaluation of discharge intensity. Images of background light were subtracted to normalize the intensities of the ICCDs.

3.4 BREAKDOWN VOLTAGES

The 50 % breakdown voltages of the different configurations were estimated using the "up-and-down" method [10] with n = 20 shots and steps of 0.5 kV. The results were corrected for pressure, temperature and humidity according to [8].

In addition to the experiments with dielectric barriers, breakdown voltages of 60-120 mm rod-plane gaps without barriers were found.

4 RESULTS

4.1 ROD-PLANE GAP WITH BARRIER UNDER POSITIVE LI

Figure 5 shows a typical positive breakdown. In frame 1, positive streamers propagate from the rod to ground, without causing breakdown. These streamers move around the barrier with ca. 2 mm/ns [22]. After the streamer propagation and crossing, a leader channel stem appears about 25 mm over the rod tip stretching horizontally out from the rod. The channel heats up sufficiently to become a leader discharge, moving in a tortuous and branched path around the barrier toward the grounded electrode. Streamers connect the leader channel tip to the ground plane, supporting a current of around 0.25–1.5 A (Figure 7).

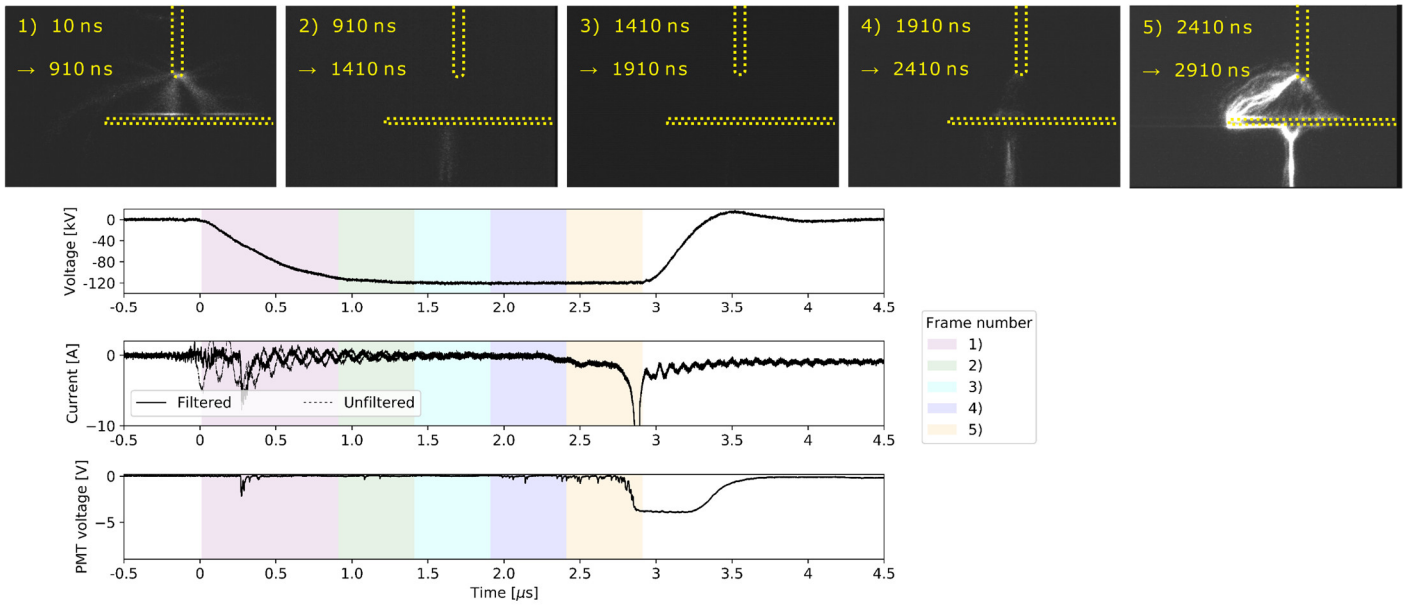

Figure 6. $d = 60$ mm rod-plane gap with barrier at $c = 40$ mm with $b = 40$ mm overhang (see Figure 2), 1.2/50μs LI -124 kV applied. PMT wavelength detection range 360-650 nm with paper filter.

The current during the initial streamer discharges is around 4 A with a rise and fall time of around 30 ns and 500 ns respectively (frame 1 and 2 in Figure 5). The leader current ramps up slowly after the dark period. There is significant light activity in the 495-850 nm range during the initial streamers. The light then fades before returning during the stem development, where a slight increase in PMT voltage is observed in the last part of the cyan color-shaded part of the graph. In the yellow and red frames 5 and 6 the PMT voltage rises close to saturation levels as the leader channel grows in length, thickness and intensity.

The positive breakdown voltages (see Figure 9) fall within the range predicted by equation (2). The positive breakdown voltages of gaps with cleaned barriers are marginally higher than those of rod-plane gaps with similar shortest paths x_S. Positive leader-type channel speeds (Figure 7) generally fall within the expected range of equation (3).

4.2 ROD-PLANE GAP WITH BARRIER UNDER NEGATIVE LI

The image series in Figures 6 and 8 confirm that negative breakdown involves a system of discharge mechanisms of both polarities. Under negative lightning impulse, the negative streamer discharges do not always seem to propagate all the way to ground (see frame 1 in Figure 6). Instead, positive streamers (frame 2) and a leader (frame 5) propagate from the grounded plane right below the rod around the barrier in Figure 6 or directly from the grounded plane to the rod as in frame 3 of Figure 8. The positive and negative streamer channels re-illuminate in frame 4 of Figure 6. The whole leader path is best seen in frame 5 of Figure 6. It starts below the rod and propagates along the lower side of the barrier. As it reaches the end of the barrier, it continues along the shortest path to the rod. Figure 8 reveals that the leader is not necessarily launched from right underneath the rod. Negative leaders were not observed, although a stem appears at the rod electrode during frame 3 in Figure 8.

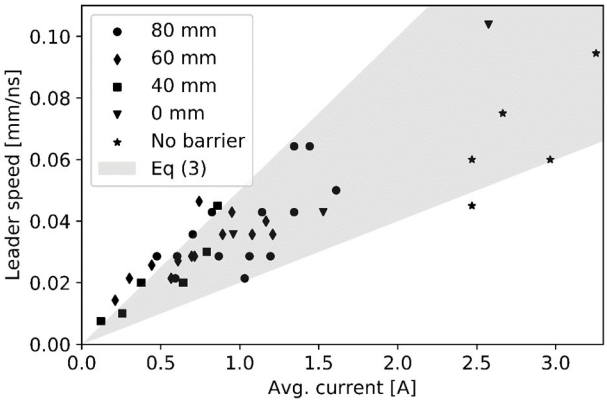

Figure 7. Positive leader speed vs. current, estimated from pictures, $d = 60$ mm rod-plane gaps with and without barrier at $c = 40$ mm (see Figure 2). 41 data points, compared with equation (2). Marker shape indicates barrier overhang b. Each point represents an image with known exposure time, such as frame 6 in Figure 5. During that frame, the leader propagates approximately 30 mm. The average current during the frame (red color-shaded area) is 1.11 A.

The current development during negative and positive LI are similar. The first current pulse during the negative streamer propagation (frame 1 in Figures 6 and 8) has similar amplitude and shape as the positive streamer pulse in Figure 5, but with opposite polarity. After a dark period, the current quickly rises to breakdown as the leader connects the plane to the rod. The over-current protection is activated at the end of frame 5 in Figure 6 and frame 3 in Figure 8. Light is recorded at the same time as the current. In Figure 6, the paper filter ensures that the PMT is not saturated before the arc phase. The PMT in Figure 8, however, is almost saturated directly during the initial streamers. The re-saturation during frame 2 indicates the inception time of the positive streamer or stem from the ground plane.

Negative breakdown voltages increase with roughly 1.2 kV/mm for gaps without barriers, and 0.9 kV/mm for gaps with

barriers (see Figure 9). These are typical field strengths required for negative streamer propagation [10].

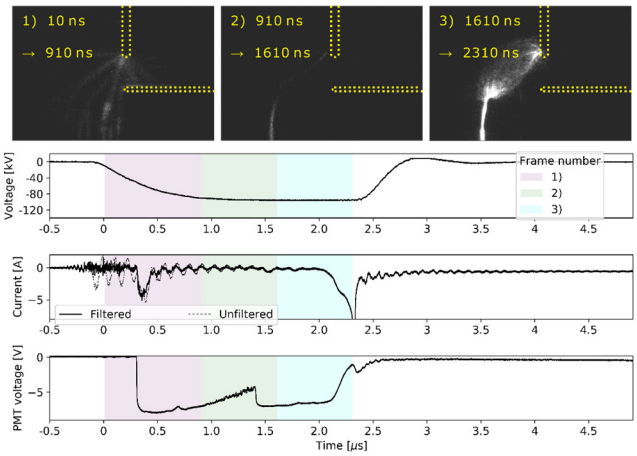

Figure 8. $d = 60$ mm rod-plane gap with barrier at $c = 40$ mm with $b = 0$ mm overhang (see Figure 2), 1.2/50µs LI -124 kV applied. PMT wavelength detection range 360-850 nm.

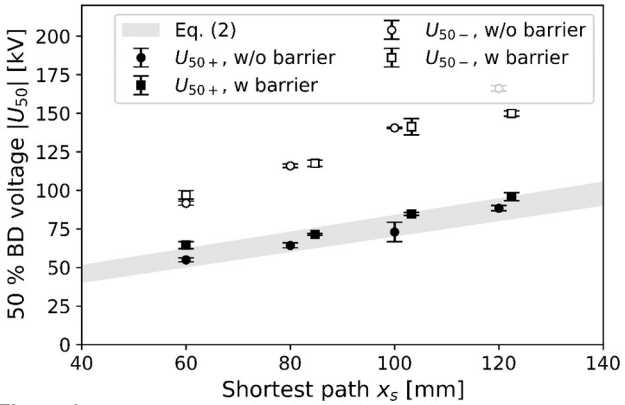

Figure 9. BD voltages as a function of shortest discharge path x_S, compared with equation (2). Error bars show 1σ standard deviation of experimental values. Round markers represent barrier-less gaps, squares gaps with barriers. Black and white color indicate positive and negative polarity respectively. All breakdowns were leader-like.

5 DISCUSSION

5.1 DISCHARGE DEVELOPMENT UNDER POSITIVE IMPULSE

Although the surface charge from initial streamers should amplify the field in the barrier-plane gap (Figure 3a), it is apparently not enough to support streamer discharges in this region. Instead, the charge shields the rod, resulting in the inception of a leader higher up on the rod, following the "leader-type channel" breakdown development described in [15].

The influence of the barrier is therefore mainly geometrical, increasing x_S (Figure 2). An additional increase in x_S is achieved as the leader inception point shifts up on the rod as in Figure 5. This shift is a result of residual charge from the initial streamers on the barrier and in the air. The effect is also seen in rod-plane gaps without barriers [19], [23], but it is more pronounced with barriers as the surface charge is less mobile than the space charge. The longer leader discharge path could explain why breakdown voltages of rod-plane gaps with dielectric barriers tend to be higher than rod-plane gaps with similar x_S (Figure 9).

It can be concluded from Figure 7 that the leader-type channels exhibit similar current-velocity relationships as leaders. This supports the view that leader discharges are not restricted to large gaps only, i.e. that leaders and "leader-type channels" are the same.

When the distance between leader and ground is short, there is more intense discharge activity at the leader front. This explains the somewhat higher average current and leader speed in gaps without a barrier, or when the barrier is at $b = 0$ mm (see Figure 7).

5.2 DISCHARGE DEVELOPMENT UNDER NEGATIVE IMPULSE

The negative charges on the barrier (see Figure 3b) cause positive streamer development from the ground plane up to the barrier. The field amplification on the ground plane is likely largest just below the rod, where the streamer starts in Figure 6. In Figure 8, however, the positive streamer starts at a distance from the barrier, to the left in the image.

Negative leaders and space stems as described in [20] are not observed, and probably require larger gaps to form. The fact that breakdown voltage is higher for negative polarity (Figure 9) is within expectations.

For a positive polarity and a given shortest discharge path x_S, the barrier measurements are associated with a slightly higher breakdown voltage than the corresponding data points of the pure air gap. The negative polarity does not show this consistency (Figure 9). A possible explanation is that the negatively charged barrier facilitates development of positive streamers and leaders from the ground plane when the barrier charge is negative.

6 CONCLUSIONS

Lightning impulse breakdown mechanisms of short rod plane air gaps with a dielectric barrier have been studied. With positive polarity applied, the breakdown mechanism constitutes positive primary streamers and the subsequent inception and propagation of a leader. Under negative impulses, negative streamers charging the barrier are followed by the inception of positive streamers propagating from the ground plane towards the barrier. A leader discharge, which propagates from the ground plane along the lower side of the barrier to the rod, is the ultimate cause of breakdown. Positive breakdown development is similar to that of leaders in larger gaps. The findings have implications for breakdown prediction models for short air gaps, which are typically based on assumptions of breakdown by streamer inception and propagation only. The dielectric barriers increase breakdown voltage by elongating the leader path and shifting the point of leader inception away from the barrier.

7 ACKNOWLEDGEMENT

This work is part of the project "Electrical insulation with low-GWP gases" (project number: 245422) funded by the

Research Council of Norway and the industrial partners ABB AS, Norway and ABB Switzerland Ltd.. The authors would also like to thank Dag Linhjell at SINTEF Energy Research, Norway, for all his help with the experimental set-up.

REFERENCES

[1] S. Solomon, D. Qin, M. Manning, Z. Chen, M. Marquis, K. B. Averyt, M. Tignor, H. L. Miller, and others, " Contribution of working group I to the fourth assessment report of the intergovernmental panel on climate change, 2007". Cambridge University Press, Cambridge, 2007.

[2] Petcharaks, Komson, "Applicability of the streamer breakdown criterion to inhomogenous gas gaps," PhD thesis, 1995, Swiss Federal Institute of Technology, Zürich

[3] A. Pedersen and A. Blaszczyk. "An Engineering Approach to Computational Prediction of Breakdown in Air with Surface Charging Effects," IEEE Trans. Dielectr. Electr. Insul., vol. 24, pp 2775-2783, 2017

[4] Z. Qiu, J. Ruan, C. Huang, W. Xu, L. Tang, D. Huang, and Y. Liao, "A method for breakdown voltage prediction of short air gaps with atypical electrodes," IEEE Trans. Dielectr. Electr. Insul., vol. 23, pp. 2685–2694, 2016.

[5] F. Mauseth, J. S. Jørstad, and A. Pedersen, "Streamer inception and propagation for air insulated rod-plane gaps with barriers," in *Annual Report IEEE Conference on Electrical Insulation and Dielectric Phenomena (CEIDP)* 2012, pp. 739–732.

[6] S. M. Lebedev, O. S. Gefle, and Y. P. Pokholkov, "The barrier effect in dielectrics: The role of interfaces in the breakdown of inhomogeneous dielectrics," IEEE Trans. Dielectr. Electr. Insul., vol. 12, pp. 537–555, Jun. 2005.

[7] T. Kouno, "Breakdown of Composite Dielectrics: The Barrier Effect," IEEE Trans. Dielectr. Electr. Insul., vol. 15,pp. 259–263, 1980.

[8] International Electrotechnical Commission, "IEC 62271-1 High voltage switchgear and controlgear Part 1: Common specifications," 2008.

[9] I. Gallimberti, "The mechanism of the long spark formation," Journal De Physique, Colloquium C, 1979, vol. 7, pp. 193–250.

[10] A. Küchler, *High Voltage Engineering: Fundamentals-Technology-Applications*. Springer, 2017.

[11] S. Singh, Y. V. Serdyuk, and R. Summer, "Streamer propagation in hybrid gas-solid insulation," in *Annual Report IEEE Conference on Electrical Insulation and Dielectric Phenomena (CEIDP)*, 2015, pp. 387–390.

[12] J. Qin and V. P. Pasko, "On the propagation of streamers in electrical discharges," J. Phys. D: Appl. Phys., vol. 47, p. 435202, 2014.

[13] G. Wormeester, S. Pancheshnyi, A. Luque, S. Nijdam, and U. Ebert, "Probing photo-ionization: Simulations of positive streamers in varying N 2 : O 2 -mixtures," J. Phys. D: Appl. Phys., vol. 43, p. 505201, 2010.

[14] G. E. Georghiou, A. P. Papadakis, R. Morrow, and A. C. Metaxas, "Numerical modelling of atmospheric pressure gas discharges leading to plasma production," J. Phys. D: Appl. Phys., vol. 38, p. R303, 2005.

[15] H. Kojima *et al.*, "Classification of impulse breakdown mechanisms under non-uniform electric field in air," IEEE Trans. Dielectr. Electr. Insul., vol. 23, no. 1, pp. 194–201, Feb. 2016.

[16] A. Haddad and D. F. Warne, *Advances in High Voltage Engineering*. IET, 2004.

[17] I. Gallimberti, G. Bacchiega, A. Bondiou-Clergerie, and P. Lalande, "Fundamental processes in long air gap discharges," Comptes Rendus Physique, vol. 3, pp. 1335–1359, 2002.

[18] A. Bondiou and I. Gallimberti, "Theoretical modelling of the development of the positive spark in long gaps," J. Phys. D: Appl. Phys., vol. 27, p. 1252, 1994.

[19] H. K. H. Meyer, F. Mauseth, A. Pedersen, M. Husøy, and J. Ekeberg, "Breakdown in short rod-plane air gaps under positive lightning impulse stress," in *Proceedings of the Nordic Insulation Symposium,* 2017.

[20] V. Cooray, *The Lightning Flash*. IET, 2003.

[21] J. E. Mark, *Polymer data handbook*. Oxford University Press, 2009.

[22] H. K. Meyer, F. Mauseth, A. Pedersen, and J. Ekeberg, "Streamer propagation in rod-plane air gaps with a dielectric barrier," in *Annual Report on IEEE Conference on Electrical Insulation and Dielectric Phenomena*, 2016, pp. 1037–1040.

[23] T. Kitamura, H. Kojima, N. Hayakawa, K. Kobayashi, T. Kato, and T. Rokunohe, "Influence of space charge by primary and secondary streamers on breakdown mechanism under non-uniform electric field in air," in *Annual Report IEEE Conference on Electrical Insulation and Dielectric Phenomena*, 2014, pp. 122–125.

[24] I. Gallimberti, G. Marchesi, and L. Niemeyer, "Streamer corona at an insulator surface," in *7th international symposium on High voltage engineering*, 1991, pp. 26–30.

[25] H. K. Meyer, F. Mauseth, A. Pedersen, and M. Husøy, "Surface charging of dielectric barriers by positive streamers," in *Annual Report IEEE Conference on Electrical Insulation and Dielectric Phenomena, 2017, pp. 802–806*

Hans Kristian Meyer received his MSc degree in Electric Power Engineering from the Norwegian University of Science and Technology (NTNU) in Trondheim, Norway. He is now a PhD Candidate at NTNU.

Frank Mauseth received his MSc degree in Electrical Engineering from Delft University of Technology, The Netherlands, in 2001. Since then he has been with the Norwegian University of Science and Technology (NTNU) in Trondheim, Norway, where he received his PhD degree in 2007 and is now an Associate Professor. Main fields of interest are high voltage insulation materials and systems, measurement methods and testing. Is currently active within the IEEE DEIS TC "HVDC Cable Systems" and CIGRÉ WG D1.48

Atle Pedersen received the M.Sc. degree and the PhD degree in electrical power engineering from the Norwegian University of Science and Technology (NTNU), Trondheim, Norway in 1994 and 2008 respectively. He has worked at ABB Distribusjon in Skien, Norway from 1994 – 2001. He has been in SINTEF Energy Research since 2006. His fields of interest include high voltage switchgear, power cables, and testing of high voltage apparatus. His research work also includes dielectric, electromagnetic and electro thermal simulations of power devices.

Jonas Ekeberg received his MSc degree in engineering physics from Uppsala University, Sweden, in 2003 and his PhD degree from Umeå University, Sweden, in 2011. He then joined ABB Corporate Research in Switzerland as a scientist with focus on high voltage insulation phenomena.